Water-soluble polysaccharides promoting production of redispersible nanocellulose

Hu, Liqiu; Xu, Wenyang; Gustafsson, Jan; Koppolu, Rajesh; Wang, Qingbo; Rosqvist, Emil; Sundberg, Anna; Peltonen, Jouko; Willför, Stefan; Toivakka, Martti; Xu, Chunlin

Published in:
Carbohydrate Polymers

DOI:
10.1016/j.carbpol.2022.119976

Published: 01/12/2022

Document Version
Accepted author manuscript

Water-soluble polysaccharides promoting production of redispersible nanocellulose

Liqiu Hu [a], Wenyang Xu [a] *, Jan Gustafsson [a], Rajesh Koppolu [a], Qingbo Wang [a], Emil Rosqvist [b], Anna Sundberg [a], Jouko Peltonen [b], Stefan Willför [a], Martti Toivakka [a], Chunlin Xu [a] *

[a] *Laboratory of Natural Materials Technology, Åbo Akademi University, Henrikinkatu 2, Turku FI-20500, Finland;*

[b] *Laboratory of Molecular Science and Engineering, Åbo Akademi University, Henrikinkatu 2, Turku FI-20500, Finland;*

**Corresponding authors: wenyang.xu@abo.fi and cxu@abo.fi*

Abstract

To date, the energy-intensive production and high-water content severely limits nanocellulose applications on a large scale off-site. In this study, adding water-soluble polysaccharides (PS) to achieve an integrated process of water-redispersible nanocellulose production was well established. The addition of PS, in particular carboxymethylated-galactoglucomannan (cm-GGM), facilitates fibre fibrillation enabling homogenization at a higher solid content at 1.5 wt% compared with around 0.4 wt% for neat fibre. More importantly, the addition of cm-GGM saved 73% energy in comparison without PS addition. Good water redispersibility of thus-prepared nanocellulose was validated in viewpoints of size distribution, morphology, viscosity and film properties as compared with neat nanocellulose. The tensile strength and optical transmittance of nanocellulose films increased to 116 MPa and 77% compared to those without PS addition of 62 MPa and 74%, respectively. Collectively, this study provides a new avenue for large-volume production of redispersible nanocellulose at a high solid content with less energy-consumption.

Keywords: Nanocellulose; water-soluble polysaccharides; redispersibility; fibre-to-fibre interaction, energy consumption decrease

1. Introduction

Fibrillated cellulosic materials are obtained by mechanically breaking millimetre-scale fibres, yielding micro- and nano- scale fibrils, *i.e.,* microfibrillated cellulose (MFC) and cellulose nanofibrils (CNF). These products possess massive specific surfaces (Yang et al., 2020), huge water-preservation ability (Sim et al., 2015) and outstanding mechanical properties (Du et al., 2019), *etc.* Most often defibrillation requiring high-intensity mechanical grinding, *e.g.,* high-pressure homogenizers, microfluidizers and grinders is an energy-intensive process (Ämmälä et al., 2021; Ang et al., 2019; Ankerfors, 2012). To decrease energy consumption, chemical and biochemical pre-treatments, such as 2,2,6,6-tetrame-thylpiperidine-1-oxyl (TEMPO) mediated oxidization, acid hydrolysis, alkaline treatment, as well as enzymatic-mediated pretreatment (Li et al., 2015; Hu et al., 2018; Lee et al., 2018; Ribeiro et al., 2019), are conducted prior to mechanical fibrillation. However, these measures cause other associated issues such as increasing cost and toxicity, and may also cause fibre degradation (Li, B et al., 2015; Isogai et al., 2011; Saito et al., 2006). Meanwhile, the highly exposed free-hydroxyl groups of the fibres, which impart good water-retention is challenging for large-scale industrial applications due to increased storage and transportation weight and space, even with a low solids content (Thomas et al., 2020). The re-dispersion of micro/nano-sized cellulose fibres in aqueous after drying is an enticing yet demanding means to address this issue. However, the irreversible aggregation of cellulose fibres during drying caused by intermolecular hydrogen bonding, *i.e.,* ‘hornification’ or ‘co-crystallization’ hamper an effective re-dispersion

process (Butchosa et al., 2014). Methods like the addition of dispersing additives/agents have been suggested to accomplish a good redispersibility, that is, in essence to disrupt 'hornification' and diminish nanofibre aggregation as well as flocculation (Butchosa et al., 2014; Dias et al., 2019; Missoum et al., 2012). However, achieving highly consistent fibrillated cellulosic products that preserves good dispersibility while imbuing them with a good redispersibility after drying is a far more demanding matter to address.

Water-soluble polysaccharides (PS) and their derivatives have been proven to intrinsically adsorb onto the fibre surface due to strong hydrogen bonds and other driving factors (Lucenius et al., 2014, 2019), interfering fibre-to-fibre interaction. Carboxymethyl cellulose (CMC) with polyelectrolyte nature has been validated as a dispersant for stabilizing MFC in suspensions by decreasing flocculation between fibres (Lowys et al., 2001), due to its irreversibly adsorption feature onto fibre surface (Laine, J et al., 2000). Moreover, CMC was found to aid the water redispersibility of cellulose nanofibrils (CNF) by introducing CMC into CNF suspension before oven drying (Butchosa et al., 2014). Controversially, several peer studies have also revealed that CMC was not necessarily absorbed onto fibres in a way (Liimatainen et al., 2019; Sorvari et al., 2014), in this case, but rather created a repulsive interaction between fibres that prevent flocculation. Essentially, the presence of PS in proximity to cellulose surface played an imperative role in serving as an inhibitor of fibre aggregation, *e.g.,* interfering interaction among fibres and reducing flocculation corresponding to enhancing water redispersibility of CNF (Albornoz-Palma et al., 2020; Dias et al., 2019; Eronen et al., 2011).

Hemicelluloses, a group of water-soluble polysaccharides considered as side-stream products in massive quantities, exhibits an intrinsic affinity to the cellulose surface (Eronen et al., 2011; Lucenius et al., 2019; Xu et al., 2019). Hemicelluloses

were found to play a role of facilitating nano-fibrillation rendering individual fibril liberation and consequently saving energy during mechanical defibrillation (Dias et al., 2019). Both Eucalyptus pulp with around 8% hemicellulose content and pine pulp containing around 10% hemicellulose content after alkaline treatment showed effective fibrillation during grinding resulting in an energy saving of 38% and 62%, respectively (Dias et al., 2019).

In the present work, an integrated approach was developed to produce water-redispersbile nanocellulose *via* homogenizing the coarsely refined pulp with the addition of polysaccharides. A wide range of water-soluble polysaccharides, *i.e.,* CMC and cationic guar gum (CGG), as well as four hemicellulose derivatives (*O*-acetyl-galactoglucomannan (GGM), cationic-GGM, anionic-GGM and xylan) were scrutinized for obtaining water-redispersible nanocellulose with good performance towards barrier applications. The effect of adding different PS on the degree of fibrillation during homogenization, as well as on water redispersibility in regards to viscosity, the optical and mechanical properties after sample re-dispersion were assessed. Addition of different PS, especially hemicelluloses, interferes fibre-to-fibre interactions during mechanical treatment, improving the defibrillation and fibre redispersibility, yielding a green and sustainable nanocellulose production.

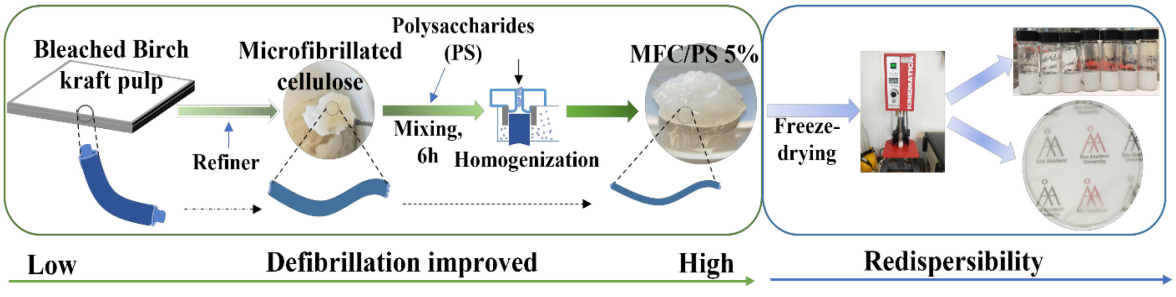

Figure 1. Schematic of processing methods to produce nanocellulose with good redispersibility

2. Experimental section

2.1. Materials

Bleached birch kraft pulp (Chemical composition: cellulose: 76.5%, hemicellulose: 21.6% determined by acid hydrolysis and acid methanolysis methods, followed by analysed gas chromatography (Sundberg et al., 1996) was kindly provided by UPM, Finland. Carboxymethyl cellulose (CMC, Mw:160 kDa) was kindly provided by CP Kelco, Finland. Cationic guar gum (CGG) was purchased from Making Cosmetics Company (U.S.A.). *O*-acetyl-galactoglucomannan (GGM, Mw: 27 kDa), cationic-GGM (cat-GGM, Mw: 45 kDa) carboxymethylated-GGM (cm-GGM, Mw: 61 kDa), and xylan (Mw: 51 kDa) were extracted in-house and syntheses were conducted according to previous works (Kisonen et al., 2014; Stevanic et al., 2014; C. Xu et al., 2010, 2011) in our group. All the molar mass of used polysaccharides are available in **Table S1**.

2.2 Methods

2.2.1. Preparation of nanocellulose from refined pulp by high-pressure homogenization

The coarsely refined pulp in terms of microfibrillated cellulose (MFC) was obtained by refining the bleached birch kraft pulp with a customized laboratory refiner, Valmet ProLab^{TM} at Åbo Akademi University.(Sjöström, 2018) Prior to refining, the pulp was soaked in water overnight for a sufficient swelling. The swollen pulp was then injected into a pulp mixer for pre-mixing at solid content of 3.5 wt%, followed by a stepwise refining process. MFC was collected when the Schopper-Riegler (°SR) value was higher than 90°.

In order to prepare nanocellulose, MFC was further mechanically treated in a high-pressure homogenizer (AH-100D, ATS Engineering Co., Ltd., China) in the absence or

presence of PS, as illustrated in **Figure 1**. Prior to homogenization, a step of rigorously mixing MFC and PS stock solutions was conducted to ensure an effective PS adsorption to the cellulose surface obtaining a homogenous slurry. The obtained slurries were passed through the homogenization chamber (the inner chamber diameter of 100 μm at 1000 bar) for 2 cycles under a pressure of approx. 200 bar followed by 10 cycles under a pressure of 1000 bar to achieve nanocellulose production. From here on in this text, we name all the nanocellulose samples as MFC/PS X%, and the mass ratio of MFC to PS is 95:5, 90:10, 85:15 and 80:20 as listed in **Table S1**, where PS stands for polysaccharide type, and X for polysaccharide concentration, as mass percentage calculated between PS and PS+MFC. The obtained products were stored at 4 °C. Moreover, in order to investigate the effects of PS on the homogenization steps, the energy consumption values were calculated by a previously described pressure drop equation (Ankerfors et al., 2012) as following: $W=\{(P_2-P_1) *1/\rho\}/c$, where W is the estimated energy consumption, in units kWh/tonne, P_1 is the atmospheric pressure, P_2 is the homogenizer pressure at 1000 bar, ρ is the density of the obtained suspension and c is the suspension solid content in weight percentage (wt%).

2.2.2. Redispersibility of MFC and MFC/PS dispersion and self-standing films

In order to assess the redispersibility of nanocellulose products, the homogenized MFC and MFC/PS samples were freeze-dried and subsequently disintegrated using a mixer (Model: PT 3000, Brinkmann Kinematica Polytron) at 20 000 rpm for 10 min. The redispersibility of the products was assessed in the forms of both dispersions and films as shown in **Figure 1**. The MFC and MFC/PS samples (5 wt%) were soaked with distilled water overnight to a final solid content of 0.4 wt% and underwent the disintegration step. In terms of MFC/cm-GGM (1–20 wt%) samples, the redispersibility studies were carried out at a solid content of 1.3 wt%. The redispersed samples were

termed as RD-MFC or RD-MFC/PS. All the redispersed samples were stored in cold room (4 ℃) prior to further use. MFC and MFC/PS samples were diluted to 0.4 wt%, followed by overnight stirring at 300 rpm to achieve a homogenous dispersion for water penetration. Suspensions with a 180 mg dry content were slowly poured into a petri dish. Subsequently, the suspensions were dried in a conditioned room (at 23 ℃ and 50% relative humidity) until reaching a constant weight. Similarly, the films preparation of redispersed samples were done using the same casting methods described above. The films were peeled off from the petri dish after drying and were stored in conditioned room prior to mechanical and optical properties tests.

2.3 Characterizations

The prepared MFC/PS dispersions and redispersibility were thoroughly characterized in the viewpoints of rheological profiles in relation to fibre-to-fibre interaction, fibre distribution via light scattering and fibre imaging analyser, nanofibre morphology change through AFM, TEM as well as SEM. The self-standing films were also cast to assess the redispersibility via film properties of their mechanical and optical properties. More characterization methodologies including sample preparation, instrument setup, and data analyses in detail are referred to **Supplementary Information**.

3. Results and discussion

3.1 One-step preparation of mechanically defibrillated nanocellulose

3.1.1 Adsorption of PS onto fibre surface achieving energy-consumption reduction

In this study, addition of hemicelluloses and their derivatives as well as other polysaccharides were established to achieve an integrated process for producing water redispersible nanocellulose with saving process energy. Firstly, when a coarsely refined

MFC-grade cellulosic material was used for producing nanocellulose through the homogenization chamber, it was observed that severe clogging issue limiting an effective production to achieve high solid content (max. 0.4 wt% prepared from Prolab^{TM} refiner). This is likely due to the high viscosity feature of MFC in course of flexible fibres and high aspect ratio (Joachim et al., 2019; Osong et al., 2016). In general, MFC suspension typically is also technically tough and energy-intensive to be homogenized when its solid content is above 2 wt% (Siró et al., 2011). Prior to homogenization step, PS was added to the coarsely refined MFC for obtaining a surface absorption to cellulose surface. It was found that the addition of hemicellulose serving as rheology modifier decreased the suspension viscosity prior to homogenization (**Figure S1a, b**), which could ease the clogging issue and facilitate the production at high solid content (higher than 1 wt%, **Table S1**) while passed through homogenizer chamber. Nevertheless, the addition amount of less than 5% is insufficient to reduce the viscosity (**Figure S1d**) to obtain an easy flow through homogenization chamber compared to MFC/PS 5 wt% (**Figure S1b**). Microscopically, sufficient adsorption of PS onto cellulose fibre surface could impart a friction reduction and strong lubrication effect among fibres (Lucenius et al., 2019). This facilitated the flowability during the homogenization steps, allowing MFC/PS to be homogenized at a higher solid content compared to the neat MFC. The benefits of the adsorbed PS on fibre surface were due to the increased repulsion force between fibres from both the charges and steric (non-ionic) stabilizing forces (Sorvari et al., 2014), consequently reducing the flocculation of cellulose micro- and nano-fibres.

The adsorption of PS onto MFC surface could also render the defibrillation along the refined fibres (Dias et al., 2019) for nanocellulose production, in particular with addition of CMC, cm-GGM, GGM, and cat-GGM (**Figure 2)**. It is intriguing to observe

196 that the MFC/cm-GGM 5% (**Figure 2d**) exhibited more fibrillation locations along
197 fibres compared to MFC/CMC 5% (**Figure 2b**). Fibre defibrillation could appear in the
198 middle of a fibre bundle with the addition of cm-GGM (as indicated by green arrow of
199 **Figure 2d**), in comparison with appearing only at the end of fibre bundle with the
200 addition of other types of PS. This can be probably related to the adsorption of PS to
201 cellulose followed by formation of mono-electric layer interfering fibre-to-fibre
202 interaction with hindering fibre aggregation (C. Xu et al., 2011). For example, the
203 charge density, *i.e.,* degree of substitution of the charged groups, in cm-GGM (DS of
204 carboxymethyl group, 1.5 (C. Xu et al., 2011)) is higher comparing to that of CMC (DS
205 of carboxymethyl group, 0.87). cm-GGM could offer greater repulsion among
206 nanofibers for better fibrillation compared with CMC. The addition of different PS to
207 the above-mentioned effect was backed up from the viewpoints of fibre-to-fibre
208 interaction through the yield stress of the produced nanocellulose suspension, where
209 the gels started flow overcoming the interaction among fibres (Magnin & Piau, 1987).
210 The relation between yield stress and shear rate of the produced nanocellulose was
211 registered in **Figure 2i**. The yield points were fitted according to Casson equation as
212 listed in **Table 1**. The adsorption of cm-GGM decreased the friction among fibres in
213 MFC with decreasing the yield stress from 0.56 Pa to 0.16 Pa, where the addition of
214 CMC showed a yield point of 0.31 Pa. This might be associated with a higher adsorption
215 amount to fibre surface of GGM (1.5 mg/m^2) than that of CMC (0.1 mg/m^2) (Eronen et
216 al., 2011; Sorvari et al., 2014).
217 Given that the benefits of enhancing defibrillation and introducing surface charge
218 interfering fibre-to-fibre interaction *via* addition of cm-GGM, different addition amount
219 of cm-GGM (1–20 wt%) was further tested to achieve successful homogenization at a
220 higher solid content at 1.5 wt%. According to Ankerfors et al (Ankerfors, 2012), the

energy consumption is inversely proportional to the feasibly homogenized solid content under the same homogenization pressure with a similar suspension density. Firstly, the feasibility of homogenizing 1.5 wt% MFC/PS was indicated by the decrease of apparent viscosity with increasing addition of cm-GGM imparting an easier flow of MFC/cm-GGM through the homogenization chamber (**Figure S1c**). This phenomenon can be speculated to the reduction of the contact friction among fibres by attaching larger amount of cm-GGM along increasing addition of cm-GGM into the system (Lucenius et al., 2014; Naidjonoka et al., 2020). As a result, the addition of cm-GGM renders a homogenization at a high solid content of 1.5 wt%. More important, the addition of 5 wt% of cm-GGM greatly decreased the energy consumption to approx. 2000 kWh/tonnes compared to homogenizing neat MFC dispersion with 0.4 wt% PS with energy-consumption of approx. 7500 kWh/tonnes (**Table S1**) – a reduction of nearly 73%.

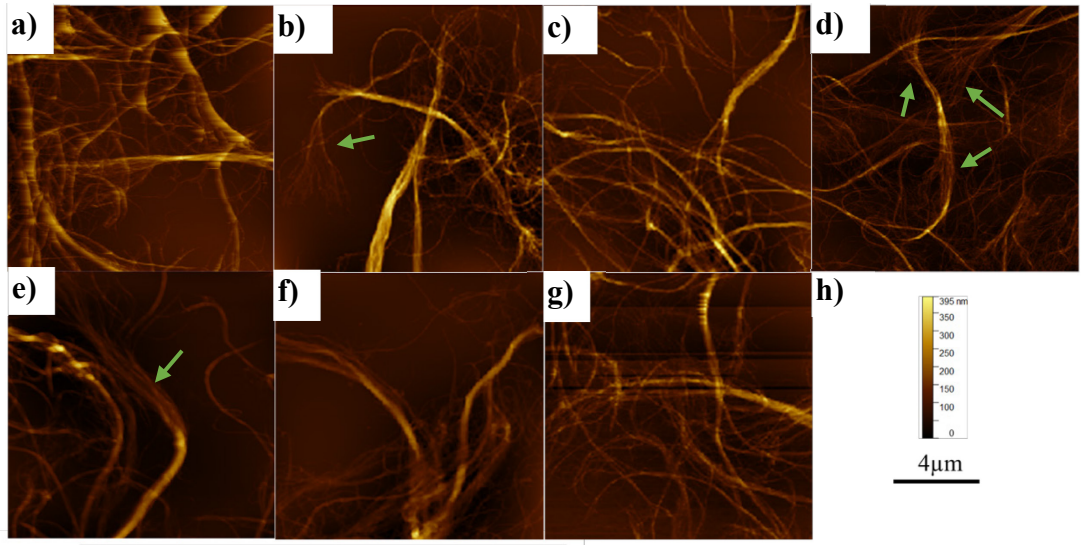

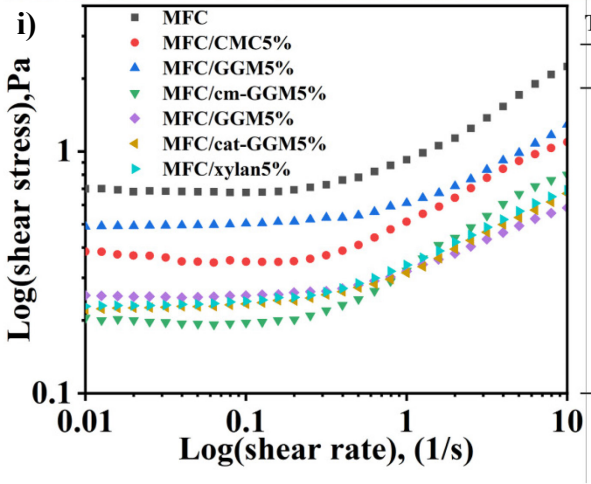

Table 1. Yield stress of MFC and MFC/PS 5% samples

Samples	Yield stress, pa
MFC	0.56
MFC/CMC 5%	0.31
MFC/CGG 5%	0.36
MFC/cm-GGM 5%	0.16
MFC/GGM 5%	0.19
MFC/cat-GGM 5%	0.17
MFC/xylan 5%	0.19

Figure 2. AFM height images of MFC and MFC/PS 5% samples: (a) MFC, (b) MFC/CMC 5%, (c) MFC/CGG 5%, (d) MFC/cm-GGM 5%, (e) MFC/GGM 5%, (f) MFC/ cat-GGM 5%, (g) MFC/xylan 5%, (h) height scale bar for all the images and (i) shear stress-shear rate profiles of MFC and MFC/PS 5% samples.

3.1.2. Size distribution and morphology of thus-prepared nanocellulose

Nanocellulose fibre size distribution in micro- and nano-scale

The effect of PS addition on fibre dimensions before and after homogenization was investigated at both micro- and nano-scale. Focusing at fibre size distribution in the range of micrometres, the addition of PS led to effective homogenization as shown by an increase of fine ratio, a decrease of length, and an increase of fibre fibrillation ratio. Most importantly, the addition of cm-GGM exhibited an outstanding properties

of presenting shortest length, and highest fine ratios of fibrillation comparing with addition of other PS (**Figure 3b**). Moreover, the addition of cm-GGM reaching the highest degree of fibrillation value of 10.56 % is also in line with the observation from AFM image (**Figure 1d**). It is further observed that the fibrillation degree was increased with the increasing addition of cm-GGM in the MFC systems (**Figure S2b**). This is possibly associated with the easy separation of fibres and repulsion of the produced nanofibers as a result of absorption of negatively charged cm-GGM onto the surface of the cellulose fibres(C. Xu et al., 2011). It is also worthwhile to stress that the effect of different additive amounts of cm-GGM on the fibre change in nanoscale by DLS (**Figure S3**) was minor from 5 to 20 wt%. Albeit that the average length of fibres was decreased with increasing addition of cm-GGM, the size of nanocellulose presenting in microscale was not further reduced when the addition of cm-GGM was above 5 wt% (**Figure S2b**).

To follow the size distribution of the produced nanocellulose in nanoscale range, DLS results mainly focus on the charge of fibre size at nanoscale (Cebreiros et al., 2021; Prakobna et al., 2015; Suopajärvi et al., 2015). It was found that the change of average size of cellulose fibrils was subtle among MFC and MFC/PS 5% blends when the suspensions were homogenized at the same low solid content of 0.4 wt%. However, introducing cm-GGM 5% to the nanocellulose suspensions resulted in the smallest average size among all PS addition (**Figure 3a**), probably due to the effective homogenization process benefited by an easier flow in the chamber and the introduced surface charge (**Figure S2a**).

Morphology of the nanocellulose with effect of polysaccharide addition

The morphological difference of nanocellulose fibres prepared by homogenization steps at the presence and absence of PS was studied with TEM. Prior to homogenization,

a number of microfibril bundles were still present in the coarsely refined MFC sample (**Figure 3c)**. After homogenization, the microfibril bundles were as-expected liberated into individual nanofibrils at the absence of PS, as observed in **Figure 3d**. With the addition of PS, the liberation of fibres tended to in the form of nanofibrils in large quantity (**Figure 3(e, f) and Figure S4 (a-c)**). This was attributed to the presence of hemicelluloses on the fibre surface hindering the fibril coalescence along with facilitating subsequent homogenization steps (Dias et al., 2019). Moreover, the microfibrils bundles were readily liberated to individual microfibrils and even elementary fibrils, as the amount of cm-GGM increased, as shown in **Figure 4 (g-j)**. It also indicated that the presence of more cm-GGM possibly resulted in a higher surface coverage and larger electrostatic repulsion among cellulose fibres.

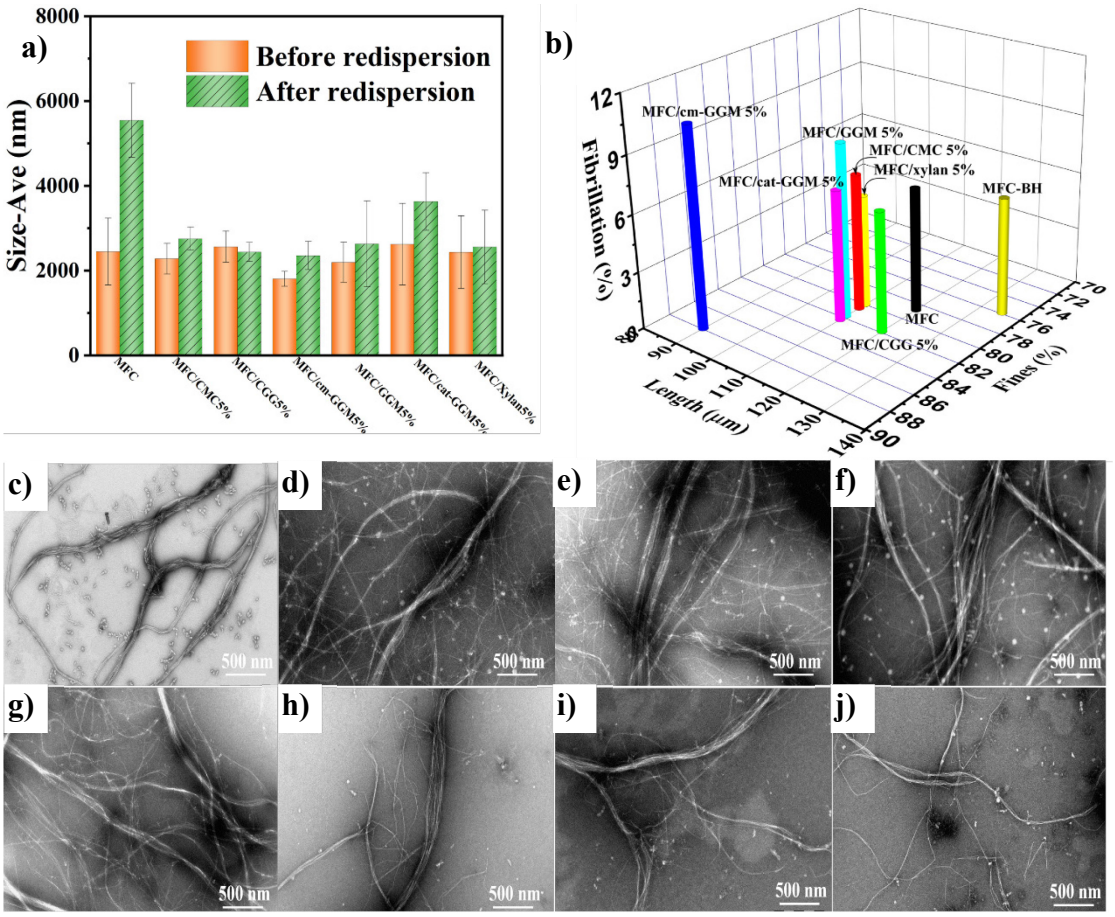

Figure 3. (a) Size average of MFC and MFC/PS 5% samples before and after redispersion; and (b) 3D plots of fibres dimension: fibre length (x axis), fine ratio (y axis) and fibrillation degree (z axis) of samples. MFC-BH: MFC prepared before homogenization. TEM images of MFC and MFC/PS 5% samples: (c) MFC before homogenization, (d-j) MFC and MFC/PS 5% after homogenization: (d) MFC, (e) MFC/CMC 5%, (f) MFC/GGM 5%, (g) MFC/cm-GGM 1%, (h) MFC/cm-GGM 5%, (i) MFC/cm-GGM 10%, (j) MFC/cm-GGM 20%.

3.2 Improving nanocellulose redispersibility through polysaccharide addition

Redispersibility is a crucial factor in nanocellulose applications with a massive quantity considering its high expense in transportation at the presence of excess water. The strong intermolecular hydrogen bonding interaction and the high surface energy of nanocellulose make it tend to aggregate during and after drying. Interfering fibre-to-fibre interaction avoiding nanofibril aggregation through approaches such as surface physical adsorption and chemical modification has been attempted to produce

redispersible nanocellulose in water or other organic solvents (Chu et al., 2020). Physical adsorption of dispersants onto nanocellulose surface is a high-efficacy approach to reduce intermolecular hydrogen bonding. Dispersants like glucose, xyloglucan, chitosan, CMC, maltodextrin, and tert-butanol have been attempted to reach nanocellulose redispersibility, as summarized in **Table 1** (Butchosa & Zhou, 2014; Hanif et al., 2018; Velásquez-Cock et al., 2018; Zhang et al., 2021). However, all the above-mentioned processes have been established after nanocellulose production where the energy consumption was initially intensive and adding process complexity.

In the following parts, the nanocellulose produced *via* addition of hemicellulose and its derivatives will be scrutinized from diverse viewpoints. Particularly, viscosity, size and morphology distribution, as well as mechanical and optical properties of the cast films of thus-prepared nanocellulose before and after redispersion were thoroughly compared.

Table 1. Comparison of among different approaches for nanocellulose redispersibility improvement

Substrates	Drying methods	Redispersing agents	Process description	Amount	Property changes	Ref.
CNF, TEMPO-CNF, CNC	Oven drying/freeze drying	Tert-butanol(t-BuOH)	a t-BuOH/water mixture remained on the cellulose surface	Water/tert-butanol (1:9, 5:5 and 9:1)	Similar in particle size, light transmittance, and sedimentation	(Hanif et al., 2018)
CNF	Oven drying	maltodextrin (MDX)	MDX/CNF mixture prevent the hornification of CNF	1-2.5-fold of nanocellulose	Similar rheological and morphological behaviour	(Velásquez-Cock et al., 2018)
CNF	Oven drying	CMC, cationic and anionic xyloglucan derivatives, chitosan (50% acetylation), hydroxyethyl cellulose	Form an interfacial film around nanocellulose and preventing aggregation	30% CMC	Lower mechanical properties	(Butchosa & Zhou, 2014)
CNC	Oven drying	Glucose	Glucose adsorption onto CNC via alcohol precipitation	20% glucose	similar particle size distribution and zeta potential	(Zhang et al., 2021)

3.2.1 Redispersibility: comparison of viscosity profile before and after redispersion

Viscosity profile is associated to fibre-to-fibre interaction and fibre-water interaction in a microscopic manner (Lowys et al., 2001). Viscosity is meanwhile an essential reflection of nanocellulose redispersibility whether reaching its initial state before drying or not.

Firstly, all the prepared nanocellulose suspensions with and without addition of PS, showed a pseudoplastic behaviour (**Figure 4a and Figure S5a**) while subjected to an increasing shear rate (Mazhari Mousavi et al., 2017; Nazari et al., 2016), featuring the related applications, e.g., in coating and extrusion, *etc*. The MFC/PS exhibited a lower viscosity profile as compared with that of homogenized MFC alone after homogenization (**Figure 4a**). It is noteworthy that the viscosity of nanocellulose (*i.e.*, MFC/cm-GGM) decreased with increasing addition amounts of cm-GGM (**Figure 4b**). This could be attributed to the introduction of surface charge onto the fibre surfaces by the PS adsorption, increasing fibre repusion. Moreover, the viscosity plateau presented at a shear rate of approximately 10 s^{-1} revealing the typical feature of thus-produced fibres in nanocellulose state, as illustrated in **Figure 4a** and **4b** (Jaiswal et al., 2021; Lowys et al., 2001; Talantikite et al., 2019). The shear flow curve exhibited the different shear rate regimes before and after the viscosity plateau due to that an addition of PS affected the inter-fibrillary structure. This is in line with the fact of PS addition interfering fibre-to-fibre interaction (**Figure 2i)**. It is also worth mentioning the apparent dip in the flow curves of all of the MFC/PS 5% suspensions at high shear rates (appearing at around 1000 s^{-1}) was outstanding as compared to the neat MFC suspension, implying a gel network structure of the produced nanocellulose with PS addition.

All the nanocellulose samples were freeze-dried and redispersed at a solid content of 0.4 wt%. **Figure 4c** and **Figure S5b** illustrated the shear-thinning behaviours of all redispersed samples under the solid content of 0.4 wt%. The viscosity of redispersed MFC was lower than the homogenized MFC suspension before redispersion in the full shear rate range. In contrast, in the presence of PS, the viscosity of redispersed MFC/PS suspension behaved similarly to the initial samples before drying possibly due to the increased ionic strength via the presence of surface charged groups, enhancing the fibre-to-fibre interactions (Agoda-Tandjawa et al., 2010). It is notable that the apparent dip at high shear rate exited in the flow curves for redispersed samples, indicating preserved gel-like network after dispersion (**Figure 4c**). In particular, both the RD-MFC/cm-GGM 5% and RD-MFC/GGM 5% enabled the recovery of nanodispersion state after drying. In addition, as the efforts to prepare water-redispersible nanocellulose in a high solid content, the drying of nanocellulose was also tested at a high solid content of 1.3 wt%. **Figure 4d** showed redispersible samples with the addition of cm-GGM (1–20%) under the solids content 1.3 wt% subjected to viscosity measurement. All samples in this case had lower viscosity (**Figure 4d**) than that prior to drying (**Figure 4b**), indicating more flocculation because of more aggregation among fibres caused by high solid content during drying.

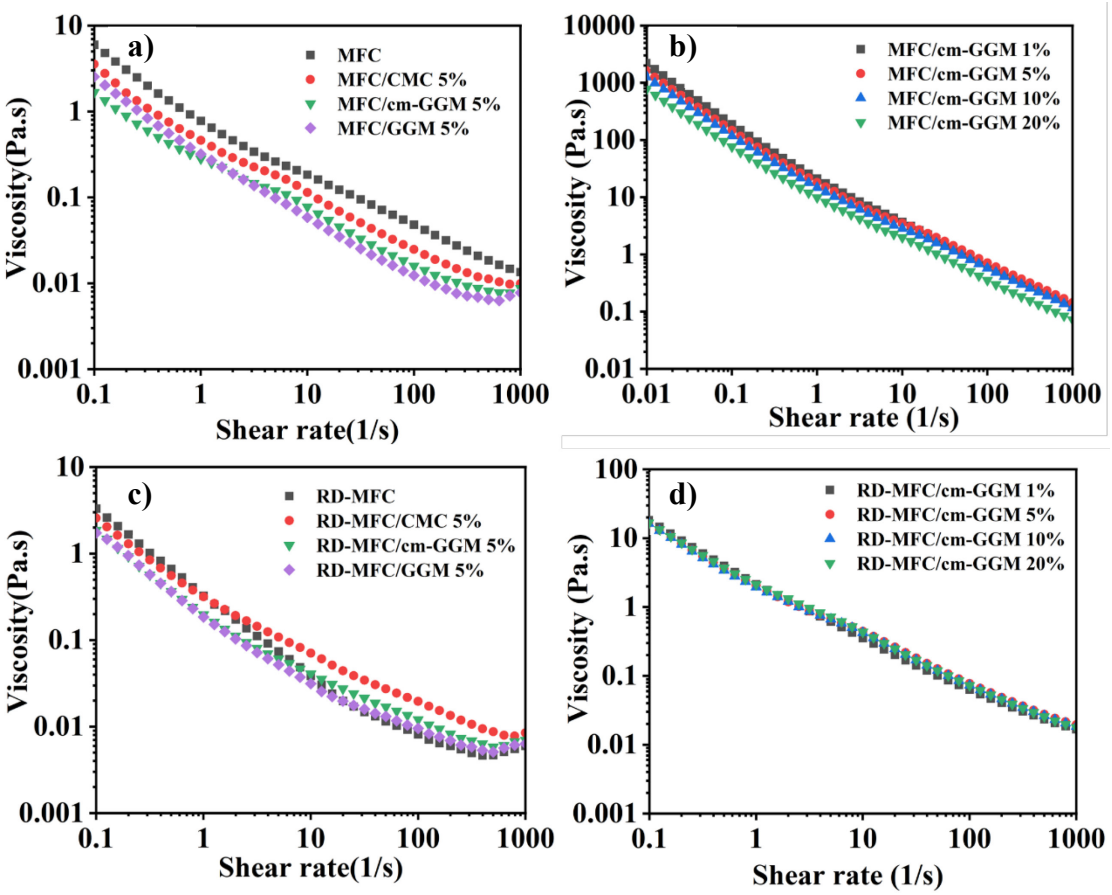

Figure 4. (a) Viscosity profile of MFC, MFC/CMC 5%, MFC.cm-GGM 5% and MFC/GGM 5% at 0.4 wt% solid content, (b) MFC/cm-GGM (1%, 5%, 10% and 20%) at 1.3 wt% solid content, (c) RD-MFC, RD-MFC/CMC 5%, RD-MFC/cm-GGM 5% and RD-MFC/GGM 5% at 0.4 wt% solid content, and (d) RD-MFC/cm-GGM (1%, 5%, 10% and 20%) at 1.3 wt% solid content.

3.2.2 Redispersibility: change of size and morphology after redispersion

The average size of the fibres in nanoscale after redispersion was examined by DLS as shown in **Figure 3a**. In comparison with the redispersed MFC, the addition of PS preserved the size distribution. This is likely due to those water-soluble hemicelluloses adsorbed on fibre surfaces facilitating fibre reorganization in water during the redispersion process (Yang et al., 2020). The addition of cm-GGM imparts the smallest fibres dimension, *i.e.,* short length, high fine ratio and large fibrillation degree, as it is comparable with that of prior to drying (**Figure S2a**). However, RD-MFC/cm-GGM (1–20%) presented a larger average size and lower fibrillation degree

at solids contents below 1.3 wt%, compared to prior to drying, particularly with 20% of cm-GGM (**Figure S3**). Furthermore, the fibres dimension of RD-MFC/cm-GGM exhibited a lower fibrillation compared to MFC/cm-GGM (**Figure S2c** and **2b**). It is notable that the average size of RD-MFC/cm-GGM 5% at a solids content of 1.3 wt% was higher than those samples at the solids content of 0.4 wt% under the same treatment condition. It could be speculated that the solids content (< 0.5 wt%) of nanocellulose suspension prior to freeze drying nanocellulose aerogel played a more dominant role than merely as redispersing aids (Huang et al., 2020; Žepič et al., 2014).

Moreover, the investigation of the morphology of fibres from the redispersed samples revealed that severe agglomeration happened in RD-MFC after freeze drying in comparison to the raw MFC suspension as a result of the strong fibre aggregation (**Figure S6a**). Intriguingly, cm-GGM with a mass fraction of 5–20 wt% resulted in a similar fibre morphology as shown in **Figure S7(f-h)**, although the fibre dimension of cm-GGM 20% observed from FS5 was comparably lower than those of cm-GGM 5% and 10%. It is assumed that nanocellulose agglomeration caused by intermolecular hydrogen bonding of cellulose fibres during drying was minimized, as the negative charges were introduced onto the surface of nanocellulose by absorbed CMC (Butchosa et al., 2014). Collectively, it was conclusive that the addition of cm-GGM for production of nanocellulose plays an imperative role on the aids of the re-defibrillation and improving redispersibility.

3.2.3 Redispersibility: film mechanical and optical properties of MFC and MFC/PS before and after redispersion

The physical properties such as density and mechanical property of the cast film are good indicators of packing nanofiber network with individual fibres or existence of flocs after redispersion (Nordenström et al., 2021). Prior to redispersion, the density of

all samples was approximately 1.3±0.1 g/cm^3 (**Table S2**). This is in the density range of nanocellulose film, 1.3-1.6 g/cm^3(Kumar et al., 2014; Nishiyama et al., 2002) confirming a very close packed structure. The tensile strength of cast films using the homogenized MFC (approx. 62 MPa), was much lower than those of MFC/PS (approx. 117 MPa), except for MFC/CMC 5% as shown in **Figure 5a**. This is possibly due to CMC acting as a plasticizer and thus enhancing the strain at break (**Table S2**) (Ninan et al., 2013). The PS derived from hemicelluloses, *i.e.*, cm-GGM, GGM, cat-GGM and xylan, significantly enhanced the tensile strength (**Table S2**) as compared to that of commercial PS. This is consistent with other reports of improving the tensile strength of CNF composites by adding hemicelluloses (Jaiswal et al., 2021; Lucenius et al., 2014). Moreover, as reported by Larsson et al. (Larsson et al., 2019), the increased defibrillation degree had a positive effect on mechanical properties *via* exposing more surface groups and binding sites of the fibres. The introduced PS can also act as physical crosslinkers (Oinonen et al., 2016; Lucenius et al., 2014, Prakobna et al., 2015) between the cellulose fibrils, which improves their mechanical properties. The effect of the additive amount of cm-GGM on the mechanical properties was further investigated (**Table S3**). It was observed that the tensile strength reached a plateau at 5 wt% addition of cm-GGM. Nevertheless, the film tensile strength of MFC/cm-GGM 5% prepared from homogenization at a solids content of 1.5 wt% was comparatively lower than at a solids content of 1 wt% (**Table S3** and **S2**). It is speculated that the slippage of nanofibrils caused by strong interfacial adhesion of cm-GGM under relatively high solids content was restricted, leading to slightly brittle films with weaker toughness, as shown in an earlier peer study (Prakobna et al., 2015). Nevertheless, the produced nanocellulose *via* the present method offers a mechanically robust film as compared with others where PS was blended with nanocellulose(Jonoobi et al., 2014; Lucenius et

al., 2019; Mikkonen et al., 2012; Nakagaito et al., 2018; Oinonen et al., 2016), as shown in **Figure 5b**.

After drying, the cast film of RD-MFC were uneven with a failure of tensile strength (**Figure 5a and Table S2)**, as observed by SEM cross-section image (**Figure S8c**). This is due to that it failed to achieve a homogeneous dispersion while it was redispersed in water. In contrast, the addition of cm-GGM supplying a high degree of fibrillation and great redispersible state allows the recovery of tensile strength for film of RD-MFC/cm-GGM. This is possibly associated to the presence of PS on the nanocellulose surface, which serves as physical link among cellulose fibrils. Those physical links could interfere the fibre-to-fibre interaction, hampering the formation of intermolecular hydrogen bonding during drying, as illustrated in **Figure 6**. Meanwhile, the presence of amorphous PS on the surface can facilitate water penetration into dried nanocellulose and thus promote fibre swelling. Moreover, the presence of surface charged PS serves as a dispersant with imparting physically adsorbed charge groups aiding the redispersion. This is also reflected by the fact that the strain at the break of films from the RD-MFC/cm-GGM 5% was slightly higher than that of RD-MFC, as agreed with the studies using TEMPO-CNFs (Sehaqui et al., 2012). In addition, it is notable that the density of all samples from RD-MFC/cm-GGM (1–20%) was decreased compared to that prior to drying (**Table S3**). This can be explained such that serious agglomeration occurred when the samples were redispersed in water, as supported by large average size (**Figure S3**), low fibre defibrillation (**Figure S2c**) and low viscosity (**Figure 4d**) compared to what was observed for the samples prior to drying. The tensile strength of MFC/cm-GGM (1-20%) did not change excessively before and after redispersion.

The optical properties of MFC films with the presence of polysaccharides were investigated as another factor revealing nanocellulose redispersibility due to that the transparency is a function of light scattering elements against nanofiber size and homogeneity(Kumar et al., 2014), as shown in **Figure 5 c, d** and **Table S2, 3**. Prior to redispersion, the transmittance rate at 550 nm of MFC films was 74%. The addition of PS, in particular cm-GGM, exhibited a slightly enhanced transparency (around 77%) with a reduction of the haze value from 83 % (haze of MFC films) to 68 %, indicating addition of cm-GGM decreasing fibre dimension(Zhao et al., 2017) after mechanical defibrillation. While mechanical defibrillation was carried out at a high solid content of 1.5 wt%, the transparency of the cast film is intriguingly increased possibly due to the feature of a less porous film associated with higher density (**Table S3**). Furthermore, after redispersion, it was observed that the transmittance rate (**Table S2**) of RD-MFC/CMC 5% and RD-MFC/cm-GGM 5% exhibited a similar transparency as those of before redispersion, supporting that fibre dimension can regain its nano-dimension. Moreover, as both the transmittance and haze rate were high, it could also be a promising coating layer in solar cells (Zhu et al., 2013). In conclusion, cm-GGM works as the best candidate among other polysaccharides achieving good water redispersibility upon assessing the redispersibility of nanocellulose in combination with the mechanical property and optical properties.

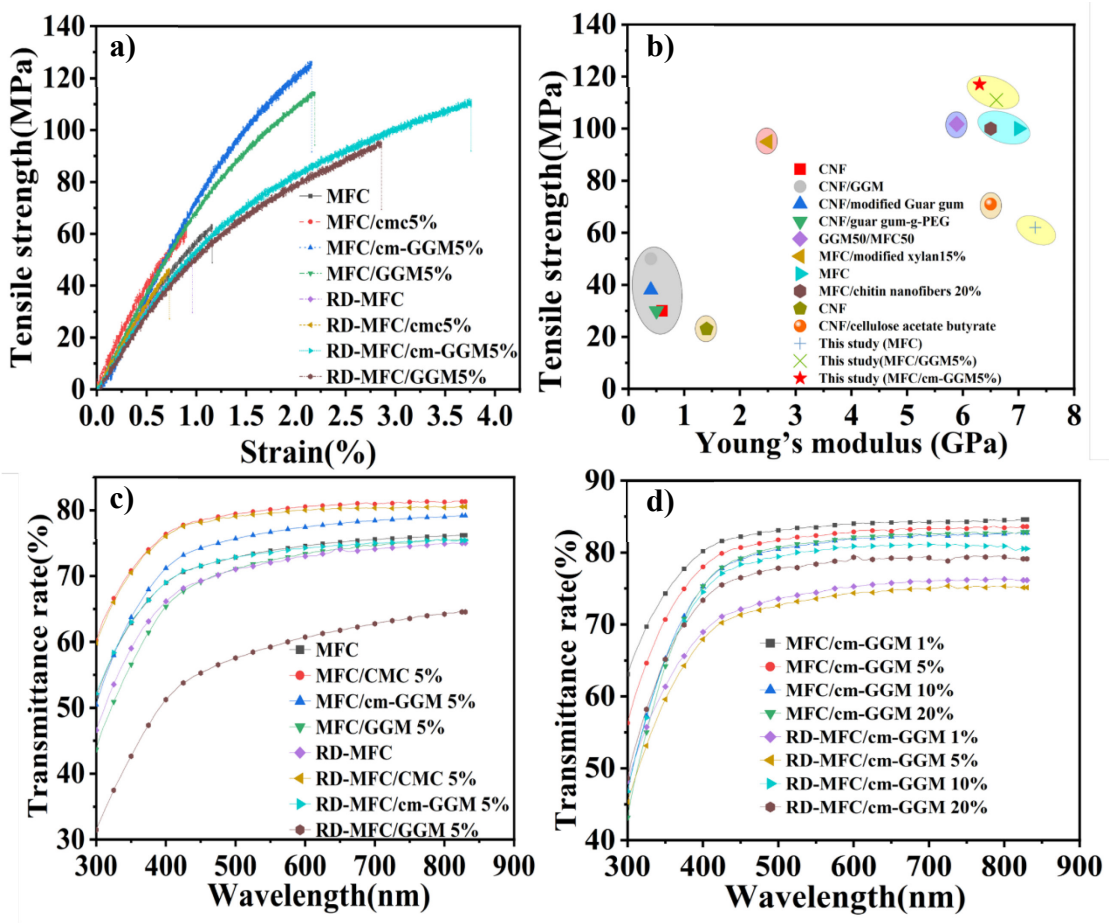

Figure 5. (a) Tensile strength of MFC, MFC/PS 5%, RD-MFC and RD/PS 5%, (b) comparison of tensile strength and Young's modulus in among peer studies and present work, (c) Optical transmittance rate of MFC, MFC/PS 5%, RD-MFC and RD-MFC/PS 5%, (d) Optical transmittance rate of MFC/cm-GGM (1%, 5%, 10%, and 20%) and RD/cm-GGM (1%, 5%, 10%, and 20%).

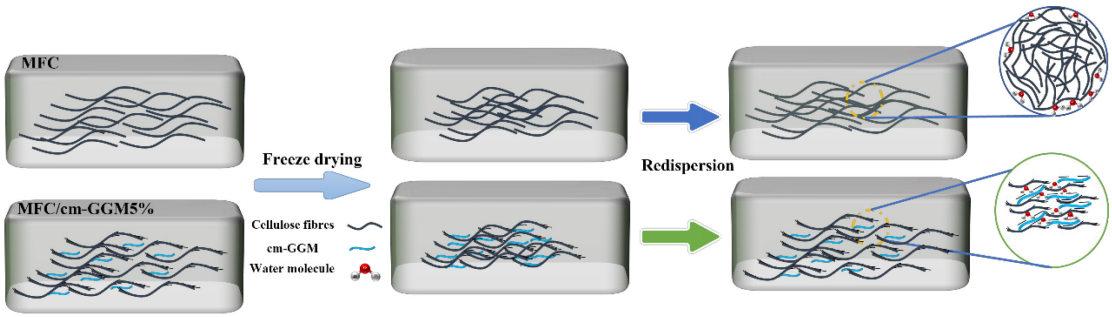

Figure 6. The proposed mechanism of interfering fibre to fibre interaction in presence of hemicellulose addition.

4. Conclusion

In the present study, an addition of six polysaccharides, *i.e.,* carboxymethyl cellulose (CMC), cationic guar gum (CGG), *O*-acetyl-galactoglucomannan (GGM), cationic-GGM, anionic-GGM, and xylan, to the coarsely refined MFC by Prolab^{TM} refiner was attempted and scrutinized to provide an integrated avenue for water-redispersible nanocellulose production. Adding PS was validated for easing the clogging issues during homogenization for nanocellulose production with significantly less energy consumption. Intriguingly, the addition of cm-GGM 5% facilitated nanocellulose production at a high solids content of 1.5 wt%, compared with a maximum of 0.4 wt% obtainable with neat MFC. Moreover, the energy consumption during nanocellulose production was considerably decreased with the addition of cm-GGM 5% prior to the homogenization steps. The addition of cm-GGM facilitated defibrillation and reduced fibre size, achieving nanocellulose production. Furthermore, the addition of cm-GGM significantly influenced the transparency and haze of nanocellulose-based films and improved their tensile strength.

In this study, it was also confirmed that an addition of PS could facilitate nanocellulose redispersibility. This can ease the transportation of nanocellulose with high solid content, reducing the transportable mass. When assessing the redispersibility, MFC/cm-GGM 5% at the solid content of 0.4 wt% exhibited a noteworthy good recovery to nano-redispersion state as was indicated in courses of viscosity, size distribution on the nano-/microscale, and tensile strength as well as film transparency. This suggests that the addition of hemicelluloses, especially cm-GGM, can improve the redispersibility of nanocellulose at low solid content. However, further studies would be required to get fully redispersible nanocellulose products at high solid content, for

instance looking into how adsorbed PS functions in the vicinity of cellulose fibre surfaces during homogenization.

Author contribution

Liqiu Hu: Methodology, Validation, Formal analysis, Writing-original draft, Visualization. Wenyang Xu: Methodology, Validation, Writing-review & editing, Supervision. Jan Gustafsson, Anna Sundberg, Martti Toivakka and Stefan Willför: Resource, Review & Editing and Supervision. Rajesh Koppolu and Qingbo Wang: Measurement and review. Emil Rosqvist and Jouko Peltonen: Resource, Review & Editing. Chunlin Xu: Conceptualization, Methodology, Resource, Review & Editing and Supervision.

Notes

The authors declare no competing financial interest.

Acknowledgement

Mr. Liqiu Hu and Mr. Qingbo Wang would like to acknowledge the financial support from the China Scholarship Council (Student ID 201908120107 for Liqiu Hu and Student ID 201907960002 for Qingbo Wang) to his doctoral study at ÅAU, Finland. All researchers in Laboratory of Natural Materials Technology are acknowledged for research assistance to support the current work. This work is also part of activities within the Johan Gadolin Process Chemistry Centre (PCC) at ÅAU.

Reference

Yang, X., Reid, M. S., Olsén, P., & Berglund, L. A. Eco-friendly cellulose nanofibrils designed by nature: effects from preserving native state. ACS Nano. 2019, 14(1), 724-735.

Sim, K., Lee, J., Lee, H., & Youn, H. J. Flocculation behavior of cellulose nanofibrils under different salt conditions and its impact on network strength and dewatering ability. Cellulose, 2015, 22(6), 3689-3700.

Du, H., Liu, W., Zhang, M., Si, C., Zhang, X., & Li, B. Cellulose nanocrystals and cellulose nanofibrils based hydrogels for biomedical applications. Carbohydr. Polym. 2019, 209, 130-144.

Ämmälä, A., Sirviö, J. A., & Liimatainen, H. Energy consumption, physical properties and reinforcing ability of microfibrillated cellulose with high lignin content made from non-delignified spruce and pine sawdust. Ind. Crops Prod. 2021, 170, 113738.

Ang, S., Haritos, V., & Batchelor, W. Effect of refining andhomogenization on nanocellulose fiber development, sheet strength and energy consumption. Cellulose, 2019, 26(8), 4767-4786.

Ankerfors, M. Microfibrillated cellulose: Energy-efficient preparation techniques and key properties (Doctoral dissertation, KTH Royal Institute of Technology). 2012.

Li, B., Xu, W., Kronlund, D., Määttänen, A., Liu, J., Smått, J. H., J.P., Willfö, S., M.X., & Xu, C. Cellulose nanocrystals prepared via formic acid hydrolysis followed by TEMPO-mediated oxidation. Carbohydr. Polym. 2015, 133, 605-612.

Hu, L.; Du, H.; Liu, C.; Zhang, Y.; Yu, G.; Zhang, X.; Si, C.; Li, B.; Peng, H. Comparative Evaluation of the Efficient Conversion of Corn Husk Filament and Corn Husk Powder to Valuable Materials via a Sustainable and Clean Biorefinery Process. ACS Sustain. Chem. Eng. 2018, 7, 1327-1336.

Lee, H.; Sundaram, J.; Zhu, L.; Zhao, Y.; Mani, S. Improved Thermal Stability of Cellulose Nanofibrils Using Low-Concentration Alkaline Pretreatment. Carbohydr. Polym. 2018, 181, 506-513.

Ribeiro, R. S. A.; Pohlmann, B. C.; Calado, V.; Bojorge, N.; Pereira, N. Production of Nanocellulose by Enzymatic Hydrolysis: Trends and Challenges. Eng. Life Sci. 2019, 19,279-291.

Isogai, A., Saito, T., & Fukuzumi, H. TEMPO-oxidized cellulose nanofibers. Nanoscale, 2011, 3(1), 71-85.

Saito, T., Nishiyama, Y., Putaux, J. L., Vignon, M., & Isogai, A. Homogeneous suspensions of individualized microfibrils from TEMPO-catalyzed oxidation of native cellulose. Biomacromolecules, 2006, 7(6), 1687-1691.

Thomas, P., Duolikun, T., Rumjit, N. P., Moosavi, S., Lai, C. W., Johan, M. R. B., & Fen, L. B. Comprehensive review on nanocellulose: Recent developments, challenges and future prospects. Journal of the mechanical behavior of biomedical materials, 2020, 110, 103884.

Butchosa, N.; Zhou, Q. Water Redispersible Cellulose Nanofibrils Adsorbed with Carboxymethyl Cellulose. Cellulose, 2014, 21 (6), 4349–4358.

Dias, M. C.; Mendonça, M. C.; Damásio, R. A. P.; Zidanes, U. L.; Mori, F. A.; Ferreira, S. R.; Tonoli, G. H. D. Influence of Hemicellulose Content of Eucalyptus and

568 Pinus Fibers on the Grinding Process for Obtaining Cellulose Micro/Nanofibrils.
569 Holzforschung 2019, 73, 1035-1046.
570 Missoum, K.; Bras, J.; Belgacem, M. N. Water Redispersible Dried
571 Nanofibrillated Cellulose by Adding Sodium Chloride. Biomacromolecules 2012, 13
572 (12), 4118–4125.
573 Lucenius, J.; Parikka, K.; Österberg, M. Nanocomposite Films Based on Cellulose
574 Nanofibrils and Water-Soluble Polysaccharides. React. Funct. Polym. 2014, 85, 167–
575 174.
576 Lucenius, J.; Valle-Delgado, J. J.; Parikka, K.; Österberg, M. Understanding
577 Hemicellulose-Cellulose Interactions in Cellulose Nanofibril-Based Composites. J.
578 Colloid Interface Sci. 2019, 555, 104–114.
579 Lowys, M. P.; Desbrières, J.; Rinaudo, M. Rheological Characterization of
580 Cellulosic Microfibril Suspensions. Role of Polymeric Additives. Food Hydrocoll.
581 2001, 15 (1), 25–32.
582 Laine, J.; Lindström, T.; Nordmark, G. G.; Risinger, G. Studies on Topochemical
583 Modification of Cellulosic Fibres. Part 1. Chemical Conditions for the Attachment of
584 Carboxymethyl Cellulose onto Fibres. Nord. Pulp Pap. Res. J. 2000, 15, 520–526.
585 Liimatainen, H., Haavisto, S., Haapala, A., & Niinimäki, J. Influence of adsorbed
586 and dissolved carboxymethyl cellulose on fibre suspension dispersing, dewaterability,
587 and fines retention. BioResources 2009. 4(1), 321-340.
588 Sorvari, A.; Saarinen, T.; Haavisto, S.; Salmela, J.; Vuoriluoto, M.; Seppälä, J.
589 Modifying the Flocculation of Microfibrillated Cellulose Suspensions by Soluble
590 Polysaccharides under Conditions Unfavorable to Adsorption. Carbohydr. Polym.
591 2014, 106 (1), 283–292.
592 Albornoz-Palma, G.; Ching, D.; Valerio, O.; Mendonça, R. T.; Pereira, M. Effect
593 of Lignin and Hemicellulose on the Properties of Lignocellulose Nanofibril
594 Suspensions. Cellulose 2020, 27 10631–10647.
595 Eronen, P.; Österberg, M.; Heikkinen, S.; Tenkanen, M.; Laine, J. Interactions of
596 Structurally Different Hemicelluloses with Nanofibrillar Cellulose. Carbohydr. Polym.
597 2011, 86 (3), 1281–1290.
598 Xu, W.; Zhang, X.; Yang, P.; Långvik, O.; Wang, X.; Zhang, Y.; Cheng, F.;
599 Sterberg, M. O.¨; Willfö, S.; Xu, C. Surface Engineered Biomimetic Inks Based on UV
600 Cross-Linkable Wood Biopolymers for 3D Printing. ACS Appl. Mater. Interfaces.
601 2019. 11(13), 12389-12400.
602 Sundheq, A., Sundherg, K., Lillandt, C., & Holmhom, B. Determination of
603 hemicelluloses and pectins in wood and pulp fibres by acid methanolysis and gas
604 chromatography. Nord. Pulp Pap. Res. J. 1996, 11(4), 216-219.
605 Kisonen, V.; Xu, C.; Eklund, P.; Lindqvist, H.; Sundberg, A.; Pranovich, A.;
606 Sinkkonen, J.; Vilaplana, F.; Willför, S. Cationised O-Acetyl Galactoglucomannans:
607 Synthesis and Characterisation. Carbohydr. Polym. 2014, 99, 755–764.
608 Stevanic, J. S., Mikkonen, K. S., Xu, C., Tenkanen, M., Berglund, L., & Salmén,
609 L. Wood cell wall mimicking for composite films of spruce nanofibrillated cellulose
610 with spruce galactoglucomannan and arabinoglucuronoxylan. J. Mater. Sci. 2014,
611 49(14), 5043-5055.

612 Xu, C.; Leppänen, A. S.; Eklund, P.; Holmlund, P.; Sjöholm, R.; Sundberg, K.;
613 Willför, S. Acetylation and Characterization of Spruce (Picea Abies)
614 Galactoglucomannans. Carbohydr. Res. 2010, 345 (6), 810–816.
615 Xu, C., Eckerman, C., Smeds, A., Reunanen, M., Eklund, P. C., Sjöholm, R., &
616 Willför, S. Carboxymethylated spruce galactoglucomannans: preparation,
617 characterisation, dispersion stability, water-in-oil emulsion stability, and sorption on
618 cellulose surface. Nord. Pulp Pap. Res. J. 2011, 26(2), 1-12.
619 Sjöström, Erik. Production of microfibrillated cellulose by LC-refining. MSc
620 thesis, Åbo Akademi University, Åbo. 2018.
621 Joachim, M. S.; Patrick, S.; Mangin, G. P.; Mangin, P.; Schenker, M.; Schoelkopf,
622 Á. J.; Gane, Á. P.; Gane, P. Rheology of Microfibrillated Cellulose (MFC) Suspensions:
623 Influence of the Degree of Fibrillation and Residual Fibre Content on Flow and
624 Viscoelastic Properties. Cellulose 2019, 26, 845–860.
625 Osong, S. H.; Norgren, S.; Engstrand, P. Processing of Wood-Based
626 Microfibrillated Cellulose and Nanofibrillated Cellulose, and Applications Relating to
627 Papermaking: A Review. Cellulose, 2016, 23, 93–123.
628 Siró, I.; Plackett, D.; Hedenqvist, M.; Ankerfors, M.; Lindström, T. Highly
629 Transparent Films from Carboxymethylated Microfibrillated Cellulose: The Effect of
630 Multiple Homogenization Steps on Key Properties. J. Appl. Polym. Sci. 2011, 119 (5),
631 2652–2660.
632 Magnin, A., & Piau, J. M. Shear rheometry of fluids with a yield stress. J.
633 Nonnewton. Fluid Mech. 1987, 23, 91-106.
634 Naidjonoka, P.; Arcos Hernandez, M.; Pá, G. K.; Heinrich, F.; Stålbrand, H.;
635 Nylander, T. On the Interaction of Softwood Hemicellulose with Cellulose Surfaces in
636 Relation to Molecular Structure and Physicochemical Properties of Hemicellulose.
637 Soft Matter 2020, 16, 7063-7076.
638 Cebreiros, F., Seiler, S., Dalli, S. S., Lareo, C., & Saddler, J. Enhancing cellulose
639 nanofibrillation of eucalyptus Kraft pulp by combining enzymatic and mechanical
640 pretreatments. Cellulose 2021, 28(1), 189-206.
641 Prakobna, K.; Kisonen, V.; Xu, C.; Berglund, L. A. Strong Reinforcing Effects
642 from Galactoglucomannan Hemicellulose on Mechanical Behavior of Wet Cellulose
643 Nanofiber Gels. J. Mater. Sci. 2015, 50 (22), 7413–7423.
644 Suopajärvi, T.; Niinimäki, H. L. & J. Morphological Analyses of Some Micro-and
645 Nanofibrils from Birch and Wheat Straw Sources. J. Wood Chem. Technol. 2015, 35
646 (2), 102–112.
647 Chu, Y., Sun, Y., Wu, W., & Xiao, H. Dispersion Properties of Nanocellulose: A
648 Review. Carbohydr. Polym. 2020, 250, 116892.
649 Butchosa, N., & Zhou, Q. Water redispersible cellulose nanofibrils adsorbed with
650 carboxymethyl cellulose. Cellulose 2014, 21(6), 4349-4358.
651 Hanif, Z., Jeon, H., Tran, T. H., Jegal, J., Park, S. A., Kim, S. M.,& Oh, D. X.
652 Butanol-mediated oven-drying of nanocellulose with enhanced dehydration rate and
653 aqueous re-dispersion. J. Polym. Res. 2018, 25(3), 1-11.
654 Velásquez-Cock, J., Gañán, P., Posada, P., Castro, C., Dufresne, A., & Zuluaga,
655 R. Improved redispersibility of cellulose nanofibrils in water using maltodextrin as a
656 green, easily removable and non-toxic additive. Food Hydrocoll. 2018, 79, 30-39.

Zhang, Y., Xu, Y., Gao, M., Xiong, J., & Dai, L. Water-redispersible cellulose nanocrystals adsorption of glucose via alcohol precipitation. J. Wood Chem. Technol. 2021, 41(4), 169-176.

Mazhari Mousavi, S. M.; Afra, E.; Tajvidi, M.; Bousfield, D. W.; Dehghani-Firouzabadi, M. Cellulose Nanofiber/Carboxymethyl Cellulose Blends as an Efficient Coating to Improve the Structure and Barrier Properties of Paperboard. Cellulose 2017, 24 (7), 3001–3014.

Nazari, B.; Kumar, V.; Bousfield, D. W.; Toivakka, M. Rheology of Cellulose Nanofibers Suspensions: Boundary Driven Flow. J. Rheol. 2016, 60 (6), 1151–1159.

Jaiswal, A. K.; Kumar, V.; Khakalo, A.; Lahtinen, P.; Solin, K.; Pere, J.; Toivakka, M. Rheological Behavior of High Consistency Enzymatically Fibrillated Cellulose Suspensions. Cellulose 2021, 28, 2087-2104.

Talantikite, M.; Gourlay, A.; le Gall, S.; Cathala, B. Influence of Xyloglucan Molar Mass on Rheological Properties of Cellulose Nanocrystal/Xyloglucan Hydrogels. J. Renew. Mater. 2019, 7 (12), 1381-1390.

Agoda-Tandjawa, G., Durand, S., Berot, S., Blassel, C., Gaillard, C., Garnier, C., & Doublier, J. L. Rheological characterization of microfibrillated cellulose suspensions after freezing. Carbohydr. Polym. 2010, 8*0*(3), 677–686.

Yang, X.; Reid, M. S.; Olsén, P.; Berglund, L. A. Eco-Friendly Cellulose Nanofibrils Designed by Nature: Effects from Preserving Native State. ACS Nano. 2020, 14 (1), 724–735.

Huang, D.; Wu, M.; Wang, C.; Kuga, S.; Huang, Y.; Wu, M.; Huang, Y. Effect of Partial Dehydration on Freeze-Drying of Aqueous Nanocellulose Suspension. ACS Sustain. Chem. Eng. 2020, 8 (30), 11389–11395.

Žepič, V.; Fabjan, E.; Kasunič, M.; Korošec, R. C.; Hančič, A.; Oven, P.; Perše, L. S.; Poljanšek, I. Morphological, Thermal, and Structural Aspects of Dried and Redispersed Nanofibrillated Cellulose (NFC). Holzforschung 2014, 68 (6), 657–667.

Nordenström, M.; Kaldéus, T.; Erlandsson, J.; Pettersson, T.; Malmström, E.; Wågberg, L. Redispersion Strategies for Dried Cellulose Nanofibrils. ACS Sustain. Chem. Eng. 2021, 9 (33), 11003–11010.

Kumar, V., Bollström, R., Yang, A., Chen, Q., Chen, G., Salminen, P., & Toivakka, M. Comparison of nano-and microfibrillated cellulose films. Cellulose 2014, 21(5), 3443-3456.

Nishiyama, Y., Langan, P., & Chanzy, H. Crystal structure and hydrogen-bonding system in cellulose Iβ from synchrotron X-ray and neutron fiber diffraction. J. Am. Chem. Soc. 2002, 124(31), 9074-9082.

Ninan, N.; Muthiah, M.; Park, I. K.; Elain, A.; Thomas, S.; Grohens, Y. Pectin/Carboxymethyl Cellulose/Microfibrillated Cellulose Composite Scaffolds for Tissue Engineering. Carbohydr. Polym. 2013, 98 (1), 877–885.

Larsson, P. A., Riazanova, A. V., Ciftci, G. C., Rojas, R., Øvrebø, H. H., Wågberg, L., & Berglund, L. A. Towards optimised size distribution in commercial microfibrillated cellulose: a fractionation approach. Cellulose 2019, 26(3), 1565-1575.

Oinonen, P.; Krawczyk, H.; Ek, M.; Henriksson, G.; Moriana, R. Bioinspired Composites from Cross-Linked Galactoglucomannan and Microfibrillated Cellulose: Thermal, Mechanical and Oxygen Barrier Properties. Carbohydr. Polym. 2016, 136, 146–153.

Jonoobi, M., Aitomäki, Y., Mathew, A. P., & Oksman, K. Thermoplastic polymer impregnation of cellulose nanofibre networks: Morphology, mechanical and optical properties. Compos. Part A Appl. Sci. Manuf. 2014, 5*8*, 30–35.

Mikkonen, K. S., Pitkänen, L., Liljeström, V., Mabasa Bergström, E., Serimaa, R., Salmén, L., & Tenkanen, M. (2012). Arabinoxylan structure affects the reinforcement of films by microfibrillated cellulose. Cellulose, 19(2), 467-480.

Nakagaito, A. N., Kanzawa, S., & Takagi, H. Polylactic Acid Reinforced with Mixed Cellulose and Chitin Nanofibers—Effect of Mixture Ratio on the Mechanical Properties of Composites. J. Compos. Sci. 2018, 36(2), 1-12.

Sehaqui, H.; Ezekiel Mushi, N.; Morimune, S.; Salajkova, M.; Nishino, T.; Berglund, L. A. Cellulose Nanofiber Orientation in Nanopaper and Nanocomposites by Cold Drawing. ACS Appl. Mater. Interfaces. 2012, 4 (2), 1043-1049

Zhao, Y., Moser, C., Lindström, M. E., Henriksson, G., & Li, J. Cellulose Nanofibers from Softwood, Hardwood, and Tunicate: Preparation-Structure-Film Performance Interrelation. ACS Appl. Mater. Interfaces. 2017, 9(15), 13508–13519.

Zhu, H., Parvinian, S., Preston, C., Vaaland, O., Ruan, Z., & Hu, L. Transparent nanopaper with tailored optical properties. Nanoscale 2013, 5(9), 3787–3792.